University of Huddersfield Repository

Kollar, László E., Stepan, Gabor and Hogan, S.J.

Backlash in balancing systems using approximate spring characteristics

Original Citation

Kollar, László E., Stepan, Gabor and Hogan, S.J. (2000) Backlash in balancing systems using approximate spring characteristics. In: 3rd European Nonlinear Oscillations Conference, 8-12 August 1999, Lyngby, Denmark.

This version is available at http://eprints.hud.ac.uk/16654/

Backlash in Balancing Systems Using Approximate Spring Characteristics

L. E. Kollar, G. Stepan, S. J. Hogan

Abstract
A mechanical model of a balancing system is constructed and its stability analysis is presented. This model considers an interesting practical problem, the backlash. It appears in the system as a nonlinear spring characteristic with noncontinuous derivative. The upper equilibrium of the pendulum can be stabilized without backlash. Backlash causes oscillations around this equilibrium. Phase space diagrams are revealed based on simulations. Bifurcation analysis is carried out by the continuation method. The noncontinuous derivative of the spring characteristic causes problems during the calculation, therefore different types of approximate characteristics are used. The conditions of the existence of stable stationary and periodic solutions are determined in case of the approximate systems and conclusions are obtained for the exact piecewise linear system.

1   Introduction

Unstable equilibria of mechanical systems often have to be stabilized by control force. A number of applications can be found in this field, e.g. the bus running on icy road, the shimmying wheel or the balancing of standing and walking robots.

A typical example of stabilization of unstable equilibria is the balancing. The simplest model of balancing is that of the inverted pendulum [1-6]. The angle and the angular velocity of the pendulum are detected and a horizontal control force at the lowest point of the pendulum is determined by them in a way that the stick should be balanced at its upper position. Control parameters must be chosen from a bounded region for successful balancing. The stability conditions have been calculated and the stability chart in the plain of the control parameters has been constructed in earlier works [9].

A pendulum-cart system is considered in the subsequent chapters. The inverted pendulum and the motor displaying the control force are placed on a

cart and the motor drives one of the wheels of the cart through a teeth-belt. Controlling is executed by a computer which is situated outside this cart. Considering the backlash at the driving-wheel of the motor, the pendulum will swing with small amplitude around its equilibrium. The stability domain in the plain of the control parameters does not change, but it means the domain where the upper position of the pendulum or the oscillation around it is stable.

2 The pendulum-cart model

In order to describing a digital balancing system, the inverted pendulum is placed on a cart as it can be seen in Figure 1 [8,10]. The motor drives one of the wheels of this cart through a teeth-belt with stiffness s. The system has 3 degrees of freedom described by the general coordinates, x, φ and ψ. The angle φ of the pendulum and the displacement x of the cart are detected together with their derivatives.
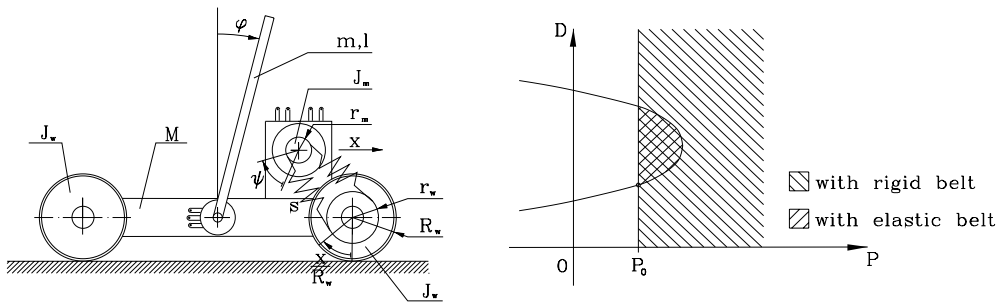

Figure 1: *The inverted pendulum on a cart and its stability map*

The control force is determined by the motor characteristic. The driving-torque is linearly proportional to the voltage U_m of the motor and to the angular velocity $\dot{\psi}$:

$$M_m = LU_m - K\dot{\psi}\,. \tag{1}$$

Considering PD controllers, we have:

$$U_m = P\varphi + D\dot{\varphi} + P_x x + D_x \dot{x}\,. \tag{2}$$

2

The system can be stabilized if the displacement of the cart is not detected ($P_x = 0$) and the differential gain D_x of the cart eliminates the damping K of the motor. Then the control force has this simplified form:

$$Q = L\left(P\varphi + D\dot{\varphi}\right) . \tag{3}$$

The system is reduced to a system with 2 degrees of freedom if a new general coordinate is introduced. This is Δ, the alongation of the spring:

$$\Delta = r_m \psi - \frac{r_w}{R_w} x . \tag{4}$$

The nonlinear equations of motion assume the form:

$$
\begin{pmatrix} \frac{(m+M)m_m r_m}{2} & -\frac{m m_m l r_m r_w \cos\varphi}{4 R_w} \\ 0 & \frac{m l^2}{3} - \frac{m^2 l^2 \cos^2\varphi}{4(m+M)} \end{pmatrix}
\begin{pmatrix} \ddot{\Delta} \\ \ddot{\varphi} \end{pmatrix}
+
\begin{pmatrix} (m+M)\frac{K}{r_m} & 0 \\ 0 & 0 \end{pmatrix}
\begin{pmatrix} \dot{\Delta} \\ \dot{\varphi} \end{pmatrix}
+
$$

$$
\begin{pmatrix} \frac{m m_m l r_m r_w}{4 R_w}\dot{\varphi}^2 \sin\varphi \\ \frac{m^2 l^2 \cos\varphi}{4(m+M)}\dot{\varphi}^2 \sin\varphi - \frac{mgl}{2}\sin\varphi \end{pmatrix}
+
\begin{pmatrix} (m+M)\,r_m + \frac{m_m r_m r_w^2}{2 R_w^2} \\ \frac{m l r_w}{2(m+M)R_w} \end{pmatrix} R_s
=
$$

$$
\begin{pmatrix} (m+M)\,Q \\ 0 \end{pmatrix} , \tag{5}
$$

where

$$
R_s = \begin{pmatrix} -s\frac{r_w}{R_w} & 0 & s r_m \end{pmatrix}
\begin{pmatrix} x \\ \varphi \\ \psi \end{pmatrix} = s\Delta \tag{6}
$$

is the force in the spring.

The stability analysis is carried out by the Routh-Hurwitz criterion. If the belt is ideally rigid, then $\Delta = 0$, x determines ψ uniquely, so the system has 2 degrees of freedom, namely x and φ. The $\varphi \equiv 0$ trivial solution of this system is asymptotically stable if and only if

$$
P > P_0 = \frac{1}{L}\left[\left(m + M + \frac{1}{2}m_m \frac{r_w^2}{R_w^2}\right) g\frac{r_m R_w}{r_w}\right] \quad \text{and} \quad D > 0 . \tag{7}
$$

If the belt is elastic, then the trivial solution of the linearized form of (5) is asymptotically stable if and only if

$$
P > P_0 \quad \text{and} \quad H_2 > 0 . \tag{8}
$$

3

where H_2 is the maximum sized Hurwitz-determinant, not presented here algebraically.

The stability chart is constructed as it is shown in Figure 1. The stability domain shrinks as the stiffness of the driving-belt decreases and at a certain critical value, it disappears. This critical value has this form:

$$s > s_{crit} = \frac{3 \left(m + M \right) m_m g}{\left(m + 4M + 2m_m \frac{r_w^2}{R_w^2} \right) l} \,.$$ (9)

3 Numerical study of the phase-space

Backlash appears in the system as a nonlinear spring characteristic. The force in the spring is the function of Δ:

$$R_s = \begin{cases} s \left(\Delta + r_0 \right) & \Delta \leq -r_0 \\ 0 & |\Delta| < r_0 \\ s \left(\Delta - r_0 \right) & \Delta \geq r_0 \end{cases} ,$$ (10)

where r_0 is the value of backlash. This function is given in Figure 2(a).
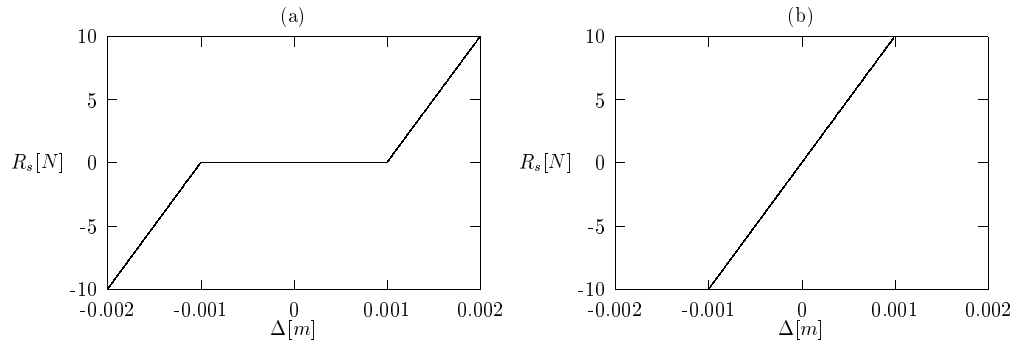

Figure 2: *(a) The piecewise linear spring characteristic at $s = 10[\frac{\text{kN}}{\text{m}}]$ and $r_0 = 1[\text{mm}]$, (b) The linear spring characteristic at $s = 10[\frac{\text{kN}}{\text{m}}]$*

New constant expressions appear in the equations of motion, that means shifting of the solutions. The stability domain does not change but it is valid only if $|\Delta| > r_0$. Otherwise, the system is just in backlash, so it cannot be stabilized, because the control force is not displayed in this little domain.

If the control parameters are chosen from the stability domain, then roots of the characteristic equation are complex numbers with negative real parts.

4

Trajectories form stable focus around the $\left(\varphi, \dot{\varphi}, \Delta, \dot{\Delta}\right) = (0, 0, \pm r_0, 0)$ equilibria.

If the system is just in backlash, then the roots of the characteristic equation are positive and negative reals. Trajectories form saddle around the $(0, 0, 0, 0)$ equilibrium.
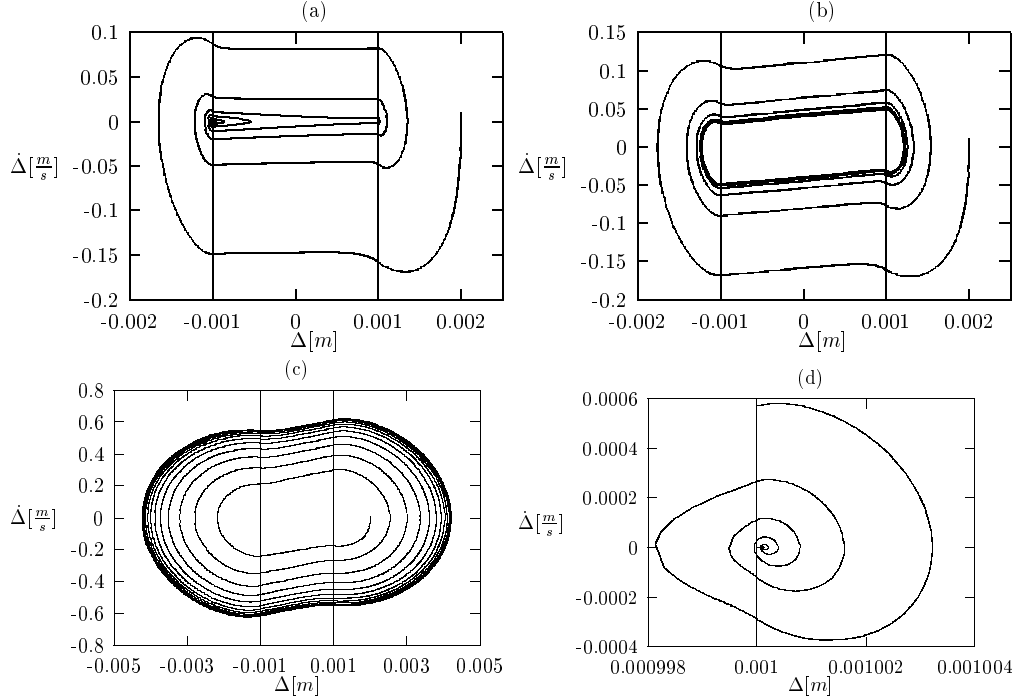

Figure 3: *Phase-diagrams on $\dot{\Delta} - \Delta$ plane, (a) $P = 2[Nm], D = 2[Nms]$, (b) $P = 20[Nm], D = 2[Nms]$, (c) $P = 100[Nm], D = 2[Nms]$, (d) $P = 20[Nm], D = 2[Nms]$ with changed initial conditions*

Simulations were accomplished using Runge-Kutta method for the study of the phase-space [7]. Results are presented in Figure 3 for the given values of parameters: $m = 0.169[kg], M = 1.136[kg], mm = 0.2[kg], g = 9.81[\frac{m}{s^2}], l = 0.5[m], r_w = 0.02[m], R_w = 0.03[m], r_m = 0.01[m], K = 0.01[Nms], s = 10000[\frac{N}{m}], r_0 = 0.001[m]$. Figure 3(a), 3(b) and 3(c) show the phase diagrams on $\dot{\Delta} - \Delta$ plane near different values of either of the control parameters, P. The $(0, 0, \pm r_0, 0)$ equilibria are stable for smaller values of P. A stable periodic solution appears for greater values of P and its amplitude is larger and larger as P increases. Its amplitude tends to infinity as P tends to the

border of the stability domain. Now the stability domain means the domain where stable stationary or periodic solution can be found.

The initial conditions are the same in these figures. They are changed in Figure 3(d) and P is the same as in Figure 3(b). The $(0, 0, r_0, 0)$ equilibrium is stable, but if P is the same as in Figure 3(c), then it becomes unstable. For certain values of P all the $(0, 0, \pm r_0, 0)$ equilibria and the limit cycle are stable and the trajectories spiral to one of them depending on the initial conditions. More investigations are needed for the exact knowledge of the phase space.

4   Approximate spring characteristics

First, the linear characteristic is considered, as if there were no backlash in the system. It is given in Figure 2(b). The bifurcation analysis is carried out by the continuation method using the (5) nonlinear equations of motion. The bifurcation diagram for $D = 2[Nms]$ is sketched in Figure 4(a). A pitchfork bifurcation is occured at $P_0 = 0.1986[Nm]$ obtained from (7), where the upper equilibrium becomes stable. It maintains its stability till the supercritical Hopf-bifurcation occured at $P_1 = 139.7[Nm]$ obtained from the Hurwitz-determinant in (8). An unstable stationary solution appears at the pitchfork bifurcation and φ tends to $\frac{\pi}{2}$ as P increases. A stable periodic solution appears at the supercritical Hopf-bifurcation and its amplitude tends to $\frac{\pi}{2}$ as P increases.
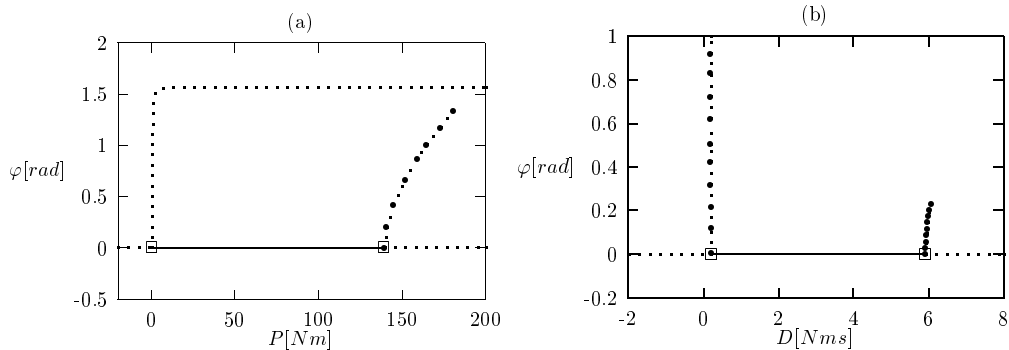

Figure 4: *Bifurcation diagram for linear spring characteristic*
(a) The bifurcation parameter is P, D = 2[Nms]
(b) The bifurcation parameter is D, P = 20[Nm]

6

The bifurcation parameter is D and $P = 20[Nm]$ in Figure 4(b). The equilibrium is stable between the Hopf-bifurcation points. They occur at $D = 0.1991[Nms]$ and $D = 5.916[Nms]$ obtained from the Hurwitz-determinant again in (8). It seems that periodic solution exists only near the border of the stability domain at this value of P.
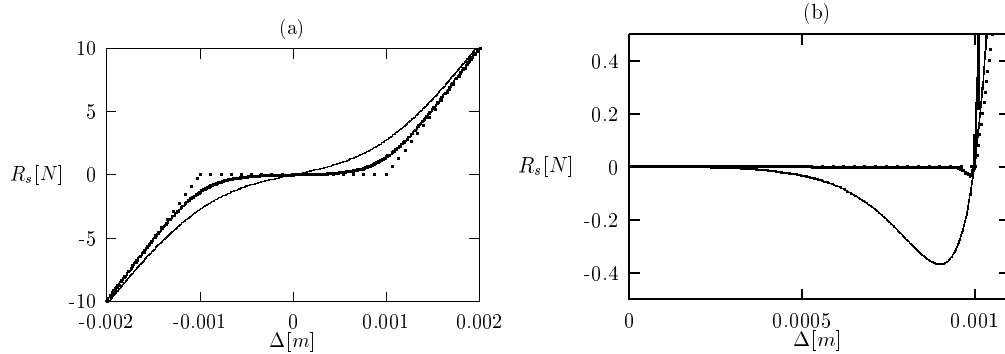

Figure 5: *Approximate spring characteristics*
(a) $R_{s1}, K_s = 2500$ (thin line), $K_s = 5000$ (thick line)
(a) $R_{s2}, K_s = 10^4$ (thin line), $K_s = 10^5$ (thick line)

Backlash means nonlinear spring characteristic with noncontinuous derivative as it is shown in Figure 2(a). Two kinds of approximation given in (11) are applied. They have more advantageous properties from view point of the calculations. The first one, R_{s1} is differentiable any times, the second one, R_{s2} is differentiable once only, but its first derivative at $\Delta = \pm r_0$ is exactly the spring stiffness s. Both of these approximations include a parameter K_s, and approximations are more and more accurate as it tends to infinity. R_{s1} and R_{s2} in the vicinity of r_0 is depicted in Figure 5(a) and 5(b) for different values of K_s.

$$R_{s1} = \frac{s}{K_s} ln \frac{1 + e^{K_s(\Delta - r_0)}}{1 + e^{-K_s(\Delta + r_0)}} \,,$$

$$R_{s2} = \begin{cases} s(\Delta + r_0) & \Delta \leq -r_0 \\ s(\Delta - r_0)e^{K_s(\Delta - r_0)} + s(\Delta + r_0)e^{-K_s(\Delta + r_0)} & |\Delta| < r_0 \\ s(\Delta - r_0) & \Delta \geq r_0 \end{cases} . \quad (11)$$
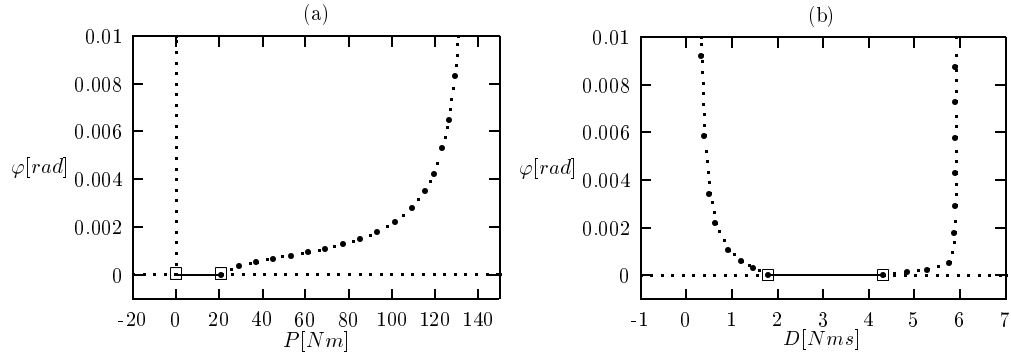
7

5   The bifurcation analysis

Figure 6: *Bifurcation diagrams using R_{s1}, $K_s = 2500$*
(a) The bifurcation parameter is P, D = 2[Nms]
(b) The bifurcation parameter is D, P = 20[Nm]
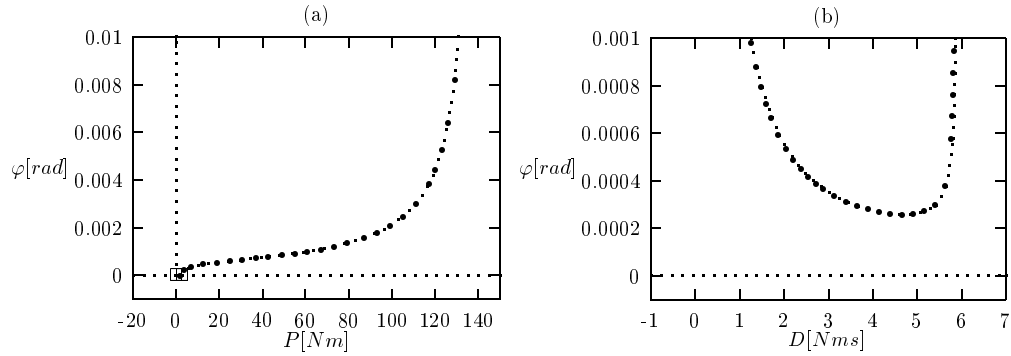

Figure 7: *Bifurcation diagrams using R_{s1}, $K_s = 5000$*
(a) The bifurcation parameter is P, D = 2[Nms]
(b) The bifurcation parameter is D, P = 20[Nm]

The bifurcation analysis in the vicinity of the upper equilibrium of the pendulum is implemented using the approximate spring characteristics. The bifurcation diagrams in case of R_{s1} are drawn in Figure 6(a), 6(b), 7(a) and 7(b). $K_s = 2500$ in Figure 6 and $K_s = 5000$ in Figure 7. The bifurcation parameter is P in Figure 6(a) and 7(a) and D in Figure 6(b) and 7(b). Changing P at a fixed value of D, the pitchfork bifurcation is found at the same P_0 where in the linear case. Increasing K_s, the Hopf-bifurcation point is closer and closer to P_0. A stable limit cycle appears at this point

and its amplitude increases as P approaches P_1, the value where the Hopf-bifurcation occured in the linear case. Changing D at a fixed value of P, two Hopf-bifurcation points are indicated in Figure 6(b). The equilibrium is stable between them, but it cannot be stabilized at the same value of P for greater K_s. Only the limit cycle is stable between the borders of the stability domain calculated in the linear case.
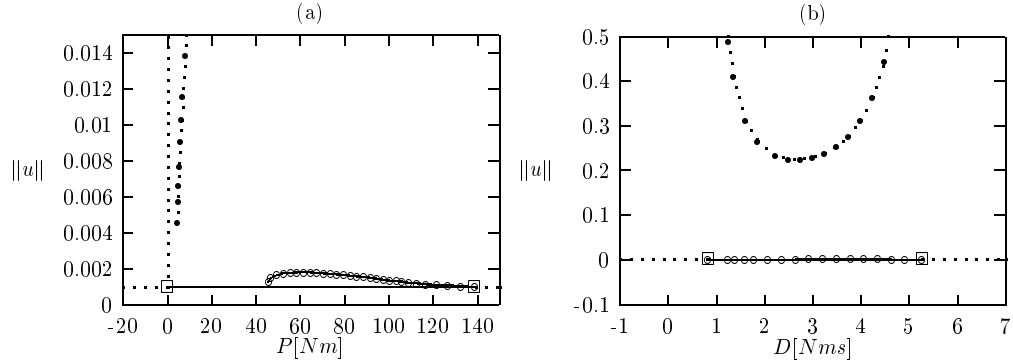

Figure 8: *Bifurcation diagrams using R_{s2}, $K_s = 10^5$*
(a) The bifurcation parameter is P, $D = 2[Nms]$
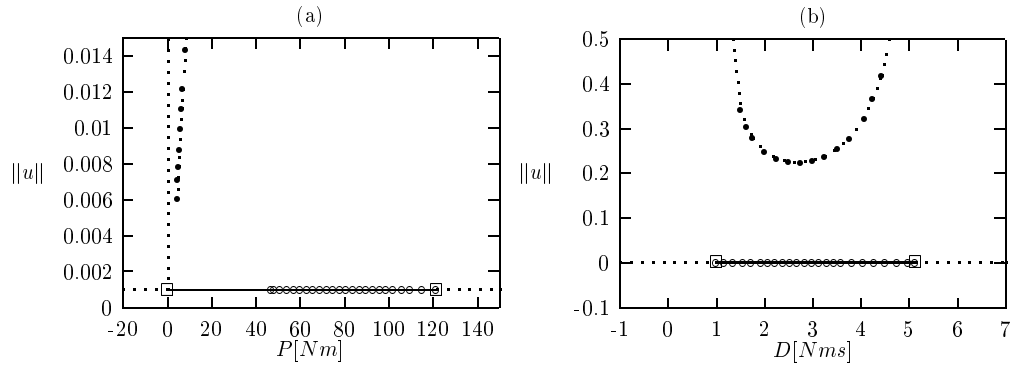*(b) The bifurcation parameter is D, $P = 75[Nm]$*

Figure 9: *Bifurcation diagrams using R_{s2}, $K_s = 3 \cdot 10^6$*
(a) The bifurcation parameter is P, $D = 2[Nms]$
(b) The bifurcation parameter is D, $P = 75[Nm]$

The bifurcation diagrams in case of R_{s2} are shown in Figure 8(a), 8(b), 9(a) and 9(b). $K_s = 10^5$ in Figure 8 and $K_s = 3 \cdot 10^6$ in Figure 9. The bifurcation parameter is P in Figure 8(a) and 9(a) and D in Figure 8(b) and

9

9(b). Changing P at a fixed value of D, the pitchfork bifurcation is found at the same P_0 where in the linear case. Increasing K_s, the Hopf-bifurcation point moves towards less values of P, but it stops at $P_2 = 69.89[Nm]$. An unstable limit cycle appears at this point and the numerical calculation is interrupted at about $P_3 = 46[Nm]$. Its amplitude tends to 0 as K_s increases. The L_2-norm of the state variables can be seen in the figures, therefore the value where the stationary solution is indicated is r_0. A bifurcation point is supposed at P_3 and the equilibrium is unstable for greater values of P. A stable limit cycle which was found with the other approximation is indicated again, but the calculation had stopped before the amplitude of the limit cycle would have decreased to 0. P is greater at the stopping point than P_0. A homoclinic orbit is showed up with simulations at this value, thus a homoclinic bifurcation is assumed here. Changing D at a fixed value of P, two Hopf-bifurcation points are indicated. The equilibrium is stable between them, but the unstable limit cycle is also found between them with decreasing amplitude as K_s increases. The stable limit cycle is also indicated here.
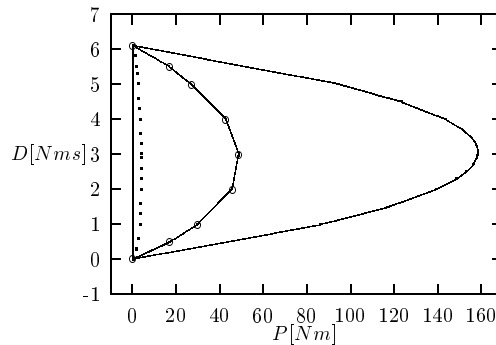

Figure 10: *The stability chart with the bifurcation curves*

Examinations are accomplished for the systems with approximate spring characteristics and conclusions can be obtained for the exact piecewise linear system, thus the stability domain in the plain of the control parameters can be constructed as it is sketched in Figure 10. It is bordered with the same straight line and parabola as it was bordered in case of the linear system (the system without backlash). Fix points are stable in a little domain near the straight line. Stable limit cycle appears at the homoclinic bifurcation point indicated with the dotted line. Fix points lose their stability at the other bifurcation point indicated with the smashed line, so all the fix points and the limit cycle are stable between the dotted and the smashed line, and only

10

the limit cycle is stable in the remaining part of the stability domain.

6   Conclusions

Backlash causes the decrease of stability domain of the equilibrium. The size of the stability domain found in case of the linear spring characteristic is the same, but a stable periodic solution exists instead of a stable stationary solution in the largest part of this domain. The physical meaning of the periodic solution is the oscillation of the stick around its vertical equilibrium. The physical meaning of the stable fix points is that the control force does not push the stick further than the vertical line and it oscillates with less and less amplitude on either side of the vertical position.

References

[1] Mori, S., Nishihara, H., Furuta, K., Control of an unstable mechanical system, *Int. J. Control* **23**, (1976) 673-692.

[2] Stépán, G., A model of balancing, *Periodica Polytechnica* **28**, (1984) 195-199.

[3] Stépán, G., *Retarded Dynamical Systems*, Longman, Harlow, UK, 1989.

[4] Henders, M. G., Sondack, A. C., 'In-the-large' behaviour of an inverted pendulum with linear stabilization, *Int. J. of Nonlinear Mechanics* **27**, (1992) 129-138.

[5] Kawazoe, Y., Manual control and computer control of an inverted pendulum on a cart, *Proc. 1st Int. Conf. on Motion and Vibration Control*, pp. 930-935, Yokohama, 1992.

[6] Enikov, E., Stépán, G., Stabilizing an Inverted Pendulum - Alternatives and Limitations, *Periodica Polytechnica*, Vol. **38**, pp. 19-26, 1994.

[7] Lóránt, G., Stépán, G., The Role of Non-Linearities in the Dynamics of a Single Railway Wheelset, *Machine Vibration* **5**, (1996) 18-26.

[8] Enikov, E., Stépán, G., Micro-Chaotic Motion of Digitally Controlled Machines, *J. of Vibration and Control*, accepted in 1997.

[9] Stépán, G., Kollár, L. E., Balancing with Reflex Delay, *Mathematical and Computer Modelling,* accepted in 1997.

[10] Kollár, L. E., Backlash in Machines Stabilized by Control Force, *Proc. of First Conference on Mechanical Engineering* pp. 147-151, Budapest, 1998.

Authors

Kollar, Laszlo E.
Department of Applied Mechanics
Budapest University of
Technology and Economics
H-1521, Budapest
Hungary
kollar@galilei.mm.bme.hu
http://www.mm.bme.hu

Hogan, S. John
Dep. of Engineering Mathematics
University of Bristol
Queen's Building, University Walk
Bristol BS8 1TR
UK
S.J.Hogan@bristol.ac.uk
http://www.fen.bris.ac.uk/engmaths

Stepan, Gabor
Department of Applied Mechanics
Budapest University of
Technology and Economics
H-1521, Budapest
Hungary
stepan@galilei.mm.bme.hu
http://www.mm.bme.hu